

Genomics

A Novel Germline Mutation in *BAP1* Predisposes to Familial Clear-Cell Renal Cell Carcinoma

Megan N. Farley^{1,2*}, Laura S. Schmidt^{8,10*}, Jessica L. Mester^{11,12}, Samuel Peña-Llopis^{1,3,4}, Andrea Pavia-Jimenez^{1,3,4}, Alana Christie¹, Cathy D. Vocke⁸, Christopher J. Ricketts⁸, James Peterson⁸, Lindsay Middleton⁸, Lisa Kinch⁵, Nick Grishin⁵, Maria J. Merino⁹, Adam R. Metwalli⁸, Chao Xing⁶, Xian-Jin Xie¹, Patricia L.M. Dahia⁷, Charis Eng^{11,12,13}, W. Marston Linehan⁸, and James Brugarolas^{1,3,4}

Abstract

Renal cell carcinoma (RCC) clusters in some families. Familial RCC arises from mutations in several genes, including the von Hippel-Lindau (VHL) tumor suppressor, which is also mutated in sporadic RCC. However, a significant percentage of familial RCC remains unexplained. Recently, we discovered that the BRCA1-associated protein-1 (*BAP1*) gene is mutated in sporadic RCC. The *BAP1* gene encodes a nuclear deubiquitinase and appears to be a classic two-hit tumor suppressor gene. Somatic *BAP1* mutations are associated with high-grade, clear-cell RCC (ccRCC) and poor patient outcomes. To determine whether *BAP1* predisposes to familial RCC, the *BAP1* gene was sequenced in 83 unrelated probands with unexplained familial RCC. Interestingly, a novel variant (c.41T>A; p.L14H) was uncovered that cosegregated with the RCC phenotype. The p.L14H variant targets a highly conserved residue in the catalytic domain, which is frequently targeted by missense mutations. The family with the novel *BAP1* variant was characterized by early-onset ccRCC, occasionally of high Fuhrman grade, and lacked other features that typify VHL syndrome. These findings suggest that *BAP1* is an early-onset familial RCC predisposing gene.

Implications: *BAP1* mutations may drive tumor development in a subset of patients with inherited renal cell cancer. *Mol Cancer Res*; 11(9); 1061–71. ©2013 AACR.

Introduction

Approximately 5% of all renal cell carcinoma (RCC) is familial (1). Several genes, including *VHL*, *MET*, *FLCN*, *FH* and genes encoding the succinate dehydrogenase (SDH)

subunits B/C/D have been identified as causative (2–4). However, the genetic basis of a significant percentage of familial RCC remains unknown. There is precedent for genes mutated in the germline (i.e., *VHL*) that are also mutated in the sporadic setting, and thus somatically mutated genes may explain familial RCC if mutated in the germline.

BAP1 (BRCA1 associated protein-1) is a tumor suppressor gene that encodes a nuclear deubiquitinase (5–7). *BAP1* functions as a classic two-hit tumor suppressor gene and is somatically mutated in uveal melanoma and mesothelioma (8, 9). Somatic mutations in *BAP1* have also been recently identified in RCC of clear cell type (ccRCC; refs. 10, 11). We found that *BAP1* is inactivated in approximately 15% of sporadic ccRCCs, and that *BAP1* mutations are associated with high Fuhrman grade and poor patient survival (11, 12).

Materials and Methods

Patient samples

Eighty-three unrelated individuals with a predisposition to RCC defined as early-onset RCC, multifocal or bilateral tumors, and/or a family history of RCC were analyzed. Peripheral blood samples were obtained from UT Southwestern Medical Center (UTSW, Dallas, TX; *n* = 6), UT Health Science Center at San Antonio (UTHSCSA, San Antonio, TX; *n* = 4), Cleveland Clinic

Authors' Affiliations: ¹Simmons Comprehensive Cancer Center; Departments of ²Clinical Genetics, ³Internal Medicine, ⁴Developmental Biology, and ⁵Biochemistry; ⁶McDermott Center for Human Growth and Development, University of Texas Southwestern Medical Center, Dallas; ⁷Department of Medicine, Cancer Therapy and Research Center, University of Texas Health Science Center at San Antonio, San Antonio, Texas; ⁸Urologic Oncology Branch, Center for Cancer Research; ⁹Translational Surgical Pathology, Laboratory of Pathology, National Cancer Institute, NIH, Bethesda; ¹⁰Basic Science Program, SAIC-Frederick, Inc., Frederick National Laboratory for Cancer Research, Frederick, Maryland; ¹¹Genomic Medicine Institute and Lerner Research Institute; ¹²Taussig Cancer Institute, Cleveland Clinic; and ¹³Department of Genetics and Genome Sciences and CASE Comprehensive Cancer Center, Case Western Reserve University School of Medicine, Cleveland, Ohio

Note: Supplementary data for this article are available at Molecular Cancer Research Online (<http://mcr.aacrjournals.org/>).

M.N. Farley and L.S. Schmidt contributed equally to this work.

Corresponding Authors: W. Marston Linehan, Urologic Oncology Branch, National Cancer Institute, Bldg 10 CRC 1W5940, Bethesda, MD 20892. Phone: 301-496-6353; Fax: 301-402-0922; E-mail: WML@nih.gov and James Brugarolas, University of Texas Southwestern Medical Center, 5323 Harry Hines Blvd., Dallas, TX 75390. Phone: 214-648-4059; Fax: 214-648-1960; E-mail: james.brugarolas@utsouthwestern.edu

doi: 10.1158/1541-7786.MCR-13-0111

©2013 American Association for Cancer Research.

Table 1. Clinical and pathologic characteristics for probands by institution

	UTSW (n = 6)	UTHSCSA (n = 4)	Cleveland (n = 26)	NCI (n = 47)	Total (n = 83)
Gender					
Male	4/6 (67%)	2/4 (50%)	7/26 (27%)	29/47 (62%)	42/83 (51%)
Female	2/6 (33%)	2/4 (50%)	19/26 (73%)	18/47 (38%)	41/83 (49%)
Race					
Caucasian	6/6 (100%)	4/4 (100%)	20/23 (87%)	40/47 (85%)	70/80 (88%)
Asian	0/6 (0%)	0/4 (0%)	1/23 (4%)	3/47 (6%)	4/80 (5%)
African-American	0/6 (0%)	0/4 (0%)	0/23 (0%)	2/47 (4%)	2/80 (3%)
American-Indian	0/6 (0%)	0/4 (0%)	1/23 (4%)	0/47 (0%)	1/80 (1%)
Other	0/6 (0%)	0/4 (0%)	1/23 (4%)	2/47 (4%)	3/80 (4%)
Ethnicity					
Hispanic	1/6 (17%)	2/4 (50%)	2/21 (10%)	1/46 (2%)	6/77 (8%)
Non-Hispanic	5/6 (83%)	2/4 (50%)	19/21 (90%)	45/46 (98%)	71/77 (92%)
Mean Age at Dx (range)	49.7 (24–70)	48.3 (26–59)	54.5 (30–79)	52.2 (33–75)	52.5 (24–79)
Laterality					
Right	5/6 (83%)	1/2 (50%)	9/18 (50%)	18/47 (38%)	33/73 (45%)
Left	1/6 (17%)	0/2 (0%)	8/18 (44%)	15/47 (32%)	24/73 (33%)
Bilateral	0/6 (0%)	1/2 (50%)	1/18 (6%)	14/47 (30%)	16/73 (22%)
Focality					
Unifocal	5/5 (100%)	2/2 (100%)	14/17 (82%)	28/47 (60%)	49/71 (69%)
Multifocal	0/5 (0%)	0/2 (0%)	3/17 (18%)	19/47 (40%)	22/71 (31%)
Histology					
Clear cell	6/6 (100%)	3/3 (100%)	12/17 (71%)	47/47 (100%)	68/73 (93%)
Papillary	0/6 (0%)	0/3 (0%)	1/17 (6%)	0/47 (0%)	1/73 (1%)
Chromophobe	0/6 (0%)	0/3 (0%)	1/17 (6%)	0/47 (0%)	1/73 (1%)
Oncocytic	0/6 (0%)	0/3 (0%)	1/17 (6%)	0/47 (0%)	1/73 (1%)
Transitional cell	0/6 (0%)	0/3 (0%)	1/17 (6%)	0/47 (0%)	1/73 (1%)
Tubulopapillary	0/6 (0%)	0/3 (0%)	1/17 (6%)	0/47 (0%)	1/73 (1%)
Fuhrman grade					
1	0/3 (0%)	0/1 (0%)	3/15 (20%)	2/45 (4%)	5/64 (8%)
2	1/3 (33%)	0/1 (0%)	8/15 (53%)	35/45 (78%)	44/64 (69%)
3	2/3 (67%)	0/1 (0%)	2/15 (13%)	5/45 (11%)	9/64 (14%)
4	0/3 (0%)	1/1 (100%)	2/15 (13%)	3/45 (7%)	6/64 (9%)
Mean tumor size (range)	5.9 (3.3–8.0)		4.4 (1.5–10.0)	5.1 (1.2–14.5)	5.0 (1.2–14.5)
pT					
1	3/5 (60%)	0/1 (0%)	12/17 (71%)	31/47 (66%)	46/70 (66%)
2	0/5 (0%)	0/1 (0%)	2/17 (12%)	9/47 (19%)	11/70 (16%)
3	2/5 (40%)	0/1 (0%)	3/17 (18%)	6/47 (13%)	11/70 (16%)
4	0/5 (0%)	1/1 (100%)	0/17 (0%)	1/47 (2%)	2/70 (3%)
pN					
0	1/2 (50%)	1/1 (100%)	2/2 (100%)	9/10 (90%)	13/15 (87%)
1	1/2 (50%)	0/1 (0%)	0/2 (0%)	1/10 (10%)	2/15 (13%)
M					
0	3/3 (100%)		2/2 (100%)	37/47 (79%)	42/52 (81%)
1	0/3 (0%)		0/2 (0%)	10/47 (21%)	10/52 (19%)
Other tumors (proband)					
Breast	0/6 (0%)	0/4 (0%)	11/26 (42%)	0/47 (0%)	11/83 (13%)
Thyroid	0/6 (0%)	0/4 (0%)	6/26 (23%)	4/47 (9%)	10/83 (12%)
Prostate	0/6 (0%)	0/4 (0%)	0/26 (0%)	3/47 (6%)	3/83 (4%)
Uterus	0/6 (0%)	0/4 (0%)	2/26 (8%)	0/47 (0%)	2/83 (2%)
Thymoma	0/6 (0%)	0/4 (0%)	1/26 (4%)	1/47 (2%)	2/83 (2%)
Pancreas	1/6 (17%)	0/4 (0%)	0/26 (0%)	0/47 (0%)	1/83 (1%)

(Continued on the following page)

Table 1. Clinical and pathologic characteristics for probands by institution (Cont'd)

	UTSW (n = 6)	UTHSCSA (n = 4)	Cleveland (n = 26)	NCI (n = 47)	Total (n = 83)
Bladder	1/6 (17%)	0/4 (0%)	0/26 (0%)	0/47 (0%)	1/83 (1%)
Esophagus	1/6 (17%)	0/4 (0%)	0/26 (0%)	0/47 (0%)	1/83 (1%)
Ovary	0/6 (0%)	0/4 (0%)	1/26 (4%)	0/47 (0%)	1/83 (1%)
Cervix	0/6 (0%)	0/4 (0%)	1/26 (4%)	0/47 (0%)	1/83 (1%)
Lung	0/6 (0%)	0/4 (0%)	0/26 (0%)	1/47 (2%)	1/83 (1%)
Pheochromocytoma	0/6 (0%)	2/4 (50%)	0/26 (0%)	0/47 (0%)	2/83 (2%)
Melanoma	0/6 (0%)	0/4 (0%)	1/26 (4%)	1/47 (2%)	2/83 (2%)
Paranglioma	0/6 (0%)	1/4 (25%)	0/26 (0%)	0/47 (0%)	1/83 (1%)
Carcinoid	0/6 (0%)	0/4 (0%)	0/26 (0%)	1/47 (2%)	1/83 (1%)
Familial RCC					
First-degree relatives					
0	4/6 (67%)	2/4 (50%)	13/26 (50%)	10/47 (21%)	29/83 (35%)
1	0/6 (0%)	2/4 (50%)	13/26 (50%)	28/47 (60%)	43/83 (52%)
2	2/6 (33%)	0/4 (0%)	0/26 (0%)	6/47 (13%)	8/83 (10%)
3	0/6 (0%)	0/4 (0%)	0/26 (0%)	3/47 (6%)	3/83 (4%)
Second-degree relatives					
0	5/6 (83%)	4/4 (100%)	14/26 (54%)	29/47 (62%)	52/83 (63%)
1	1/6 (17%)	0/4 (0%)	12/26 (46%)	12/47 (26%)	25/83 (30%)
2	0/6 (0%)	0/4 (0%)	0/26 (0%)	6/47 (13%)	6/83 (7%)
Germline mutation testing ^a					
<i>VHL</i>	6/6 (100%)	4/4 (100%)	2/26 (8%)	22/47 (47%)	34/83 (41%)
<i>SDHB</i>	0/6 (0%)	4/4 (100%)	12/26 (46%)	19/47 (40%)	35/83 (42%)
<i>SDHC</i>	0/6 (0%)	0/4 (0%)	11/26 (42%)	19/47 (40%)	30/83 (36%)
<i>SDHD</i>	0/6 (0%)	0/4 (0%)	11/26 (42%)	19/47 (40%)	30/83 (36%)
<i>PTEN</i>	0/6 (0%)	0/4 (0%)	25/26 (96%)	1/47 (2%)	26/83 (31%)
<i>BRCA1/2</i>	0/6 (0%)	0/4 (0%)	5/26 (19%)	0/47 (0%)	5/83 (6%)
<i>MET</i>	0/6 (0%)	0/4 (0%)	1/26 (4%)	3/47 (6%)	4/83 (5%)
<i>FLCN</i>	0/6 (0%)	0/4 (0%)	0/26 (0%)	7/47 (15%)	7/83 (8%)
<i>FH</i>	0/6 (0%)	0/4 (0%)	0/26 (0%)	4/47 (9%)	4/83 (5%)
<i>TSC1/2</i>	0/6 (0%)	0/4 (0%)	0/26 (0%)	3/47 (6%)	3/83 (4%)

NOTE: Mean size (cm), grade, and stage were determined on the largest tumor per patient.

Abbreviations: Dx, diagnosis; pT and pN, pathologic tumor and node stage according to American Joint Committee on Cancer, 2010 edition; M, clinical metastases.

^aGermline mutation testing refers to the number of individuals tested for mutation in each indicated gene. All genetic tests were negative.

(Cleveland, OH; *n* = 26), and the National Cancer Institute (NCI, Bethesda, MD; *n* = 47; Table 1). Deidentified samples of germline DNA were provided by the different institutions for *BAP1* sequencing under a protocol approved by the UTSW Institutional Review Board (IRB). Patients from other institutions were recruited under their own IRB protocols.

DNA extraction and *BAP1* sequencing

Germline DNA extraction (UTSW samples) and sequencing were conducted as previously described (11). For *BAP1* loss of heterozygosity (LOH) studies, DNA from fresh frozen (or microdissected formalin-fixed paraffin-embedded) tumor tissue was extracted using Maxwell 16 Tissue DNA Purification Kit or Maxwell 16 FFPE Tissue LEV DNA Purification Kit (Promega). Redesigned *BAP1*

primers were used for PCR amplification and sequencing of microdissected tumor DNA: forward primer 5'-GCCTGCCTGACCATCACC and reverse primer 5'-AAGGAAAGCAGTAGGGAAGGA.

BAP1 immunohistochemistry

Five micron formalin-fixed paraffin-embedded sections were deparaffinized and blocked with methanol-30% H₂O₂. After antigen retrieval by boiling in citrate buffer, slides were incubated with monoclonal anti-*BAP1* antibody (C-4; Santa Cruz Biotechnology) diluted 1/150. Then, slides were immunostained with avidin-biotin-peroxidase complex and developed with diaminobenzidine. Harris hematoxylin was used to counterstain the slides. Nonimmune mouse immunoglobulin was used as a negative control. Expression was evaluated as positive or negative. Staining was considered

positive when more than 10% of the nuclei showed immunoreaction.

Results and Discussion

During studies that led to the discovery of somatic *BAP1* mutations in ccRCC, a germline variant (c.121G>A; p. G41S) was identified in one individual (II:1) that had two first-degree and a second-degree relative with RCC and who had previously tested negative for a *VHL* mutation (Supplementary Fig. S1; ref. 11). The variant (c.121G>A; p. G41S) was not found in the 1000 Genomes Project (13). However, cosegregation studies suggested that it was not responsible for the cancer predisposition in this family (Supplementary Fig. S1). Nevertheless, *BAP1* mutations have been previously observed in the germline where they predispose to uveal and cutaneous melanoma as well as mesothelioma (14–18). Some of these families also exhibited other tumor types, although at much lower frequencies, including RCC (16, 17). On the basis of the somatic and germline associations of *BAP1* mutations and RCC, we sought to determine whether germline *BAP1* mutations were associated with familial RCC.

We examined 83 unrelated probands with familial RCC. Phenotypic information is summarized in Table 1. The samples were predominantly from Caucasian individuals of non-Hispanic origin. The mean age at diagnosis was 52.5 years. Twenty-two percent of the individuals had bilateral

tumors, and RCC was multifocal in 31% of the individuals. Ninety-three percent of the individuals examined had RCC of clear cell type. The mean size of the largest tumor in each individual was 5 cm. Most of these tumors were pT1 (66%) and more than 75% were of low Fuhrman nuclear grade (Grade 1-2). Lymph node and distant metastases were rare (13% and 19%, respectively). Other primary tumors reported in probands included those of the breast, thyroid, and prostate. Sixty-six percent of the individuals had at least one first-degree relative with RCC, and 37% had at least one second-degree relative with the disease. Individuals in this cohort had been previously evaluated for mutations in other RCC predisposition genes. Forty-one percent had been evaluated for germline *VHL* mutations and had tested negative. A similar percentage had tested negative for germline mutation of the SDH complex genes. Thirty-one percent of the individuals had tested negative for germline *PTEN* mutations. Fewer individuals had been screened for germline mutations in a variety of other genes including *BRCA1*, *BRCA2*, *MET*, *FLCN*, *FH*, *TSC1*, and *TSC2*. In all patients, the cause of the familial RCC predisposition remained unknown.

We sequenced the *BAP1* gene in peripheral blood DNA from the 83 probands. The coding sequence and intron/exon junctions were analyzed by Sanger sequencing as previously described (11). One out of the 83 DNA samples failed to sequence. Among the rest, a high-quality sequence

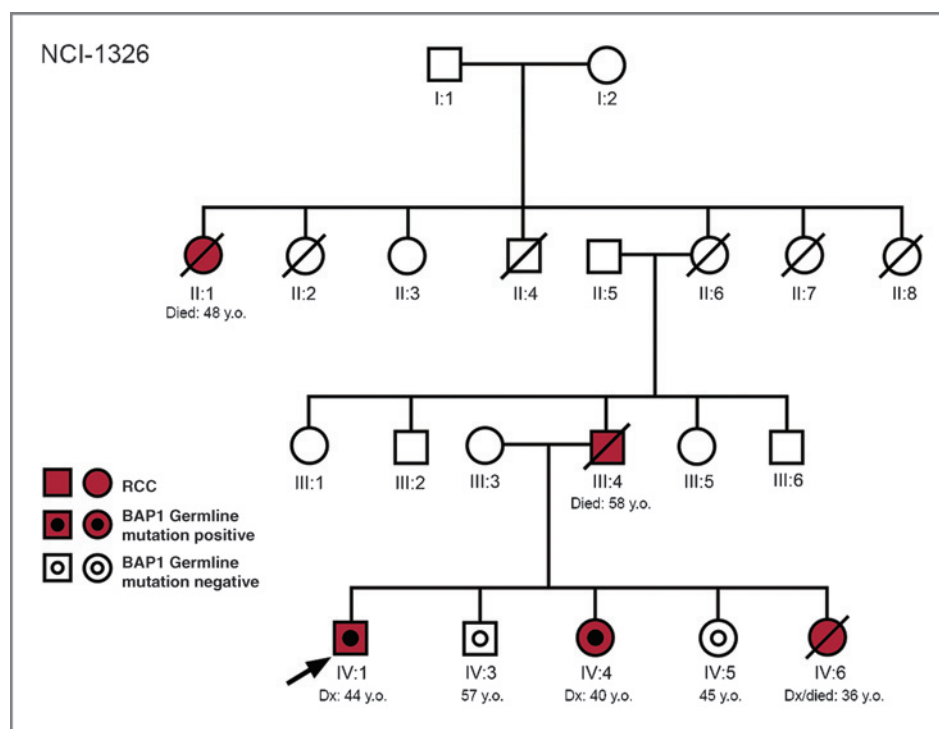


Figure 1. Family NCI-1326: an early-onset, aggressive form of bilateral, multifocal solid and cystic clear cell kidney cancer. Pedigree from familial renal cancer kindred NCI-1326. The proband IV:1 was initially diagnosed with kidney cancer at the age of 44 years. Individual IV:4 was diagnosed with RCC at the age of 40 years and individual IV:6 died of metastatic RCC at the age of 36 years. Individuals II:1 and III:4 died of metastatic RCC at 48 and 58 years of age, respectively. Two individuals with a history of RCC for whom samples were available (IV:1 and IV:4) had a germline *BAP1* variant. Two other individuals (IV:3 and IV:5) who were screened with abdominal imaging and were found to have no evidence of RCC, were negative for the germline *BAP1* gene variant. Individual IV:2 (omitted from pedigree) is the spouse of IV:1.

tracing in at least one direction was obtained for 100% of amplicons. Only two samples were detected with germline variants. A germline missense variant (c.869A>G; p.N290S) was found in a UTSW female with unilateral, unifocal ccRCC diagnosed at the age of 24 years who had previously tested negative for germline mutations in *VHL*. The variant was predicted to be benign by PolyPhen-2 (19), and conservation studies across species showed that the corresponding asparagine was replaced by a serine in some species. Thus, the variant was not analyzed further.

A second germline missense variant (c.41T>A; p.L14H) was detected in an NCI proband. This individual belonged to family NCI-1326, which included 5 individuals diagnosed with RCC. This kindred is characterized by early-onset and aggressive ccRCC. Of the 5 affected members, 3 died of metastatic kidney cancer at 36, 48, and 58 years of age (Fig. 1). The proband (IV:1) underwent a right radical nephrectomy for a multifocal RCC at the age of 44 years at an outside hospital. Pathologic evaluation revealed an 8.0 cm solid, high-grade (Fuhrman nuclear grade 3) ccRCC as well as 3 additional smaller cystic lesions with clear cell kidney cancer. In addition, an angiomyolipoma and a renal medullary fibroma were found. Because of the family history and multifocality, the patient was referred to NCI.

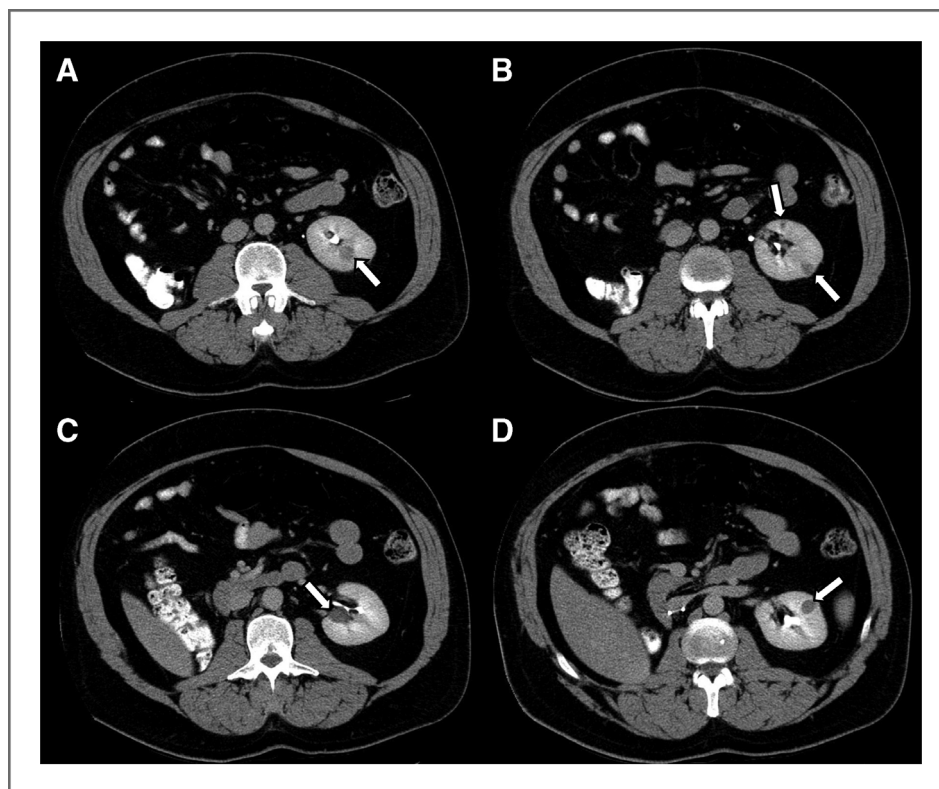
To determine the genetic basis of the RCC predisposition in this family, the proband was evaluated at the NCI for germline mutations of the following genes: *VHL*, *MET*, *FLCN*, *TSC1*, *TSC2*, *SDHB*, *SDHC*, *SDHD*, and *FH*. No germline mutations were detected in any of these genes. In

addition, germline chromosome 3 translocation familial renal carcinoma (20) was excluded by karyotype analysis.

At the NCI, the proband underwent the first of the three left partial nephrectomies at the age of 46 years. At that time, he had a resection of a 3 cm ccRCC that was found to be Fuhrman grade 3, a 1.5 cm ccRCC (also Fuhrman grade 3), and a 2 cm atypical cyst with clear cell lining (Fig. 2). Subsequently, the patient underwent active surveillance for 8 years at which point surgical intervention was recommended because of tumor growth (Fig. 3A). At the age of 54 years, when his largest renal tumor had reached 3.46 cm, he underwent a second left partial nephrectomy with removal of a ccRCC (Fuhrman grade 2) and 3 renal cysts, 2 of which were lined by "atypical clear cells" (Fig. 4A–C). The patient was then managed by active surveillance for almost 4 years. During this time, a tumor grew to 3.7 cm (Fig. 3B) necessitating a third left partial nephrectomy at the age of 57 years with removal of 4 separate ccRCCs (3 Fuhrman grade 2 and 1 Fuhrman grade 3) as well as a renal cyst. At his most current evaluation in May 2012, he had excellent renal function and was without evidence of metastatic disease.

Because of the family history, individual IV:4 underwent screening and a central mass was detected in her right kidney at the age of 40 years for which she underwent a right radical nephrectomy. This tumor was a 3.8 cm ccRCC, Fuhrman grade 2. Twelve years after the operation, she remains without evidence of disease. Individual IV:6 presented at the age of 36 years with metastatic RCC and died a short time later.

Figure 2. Bilateral, multifocal cysts and solid kidney cancer in proband IV:1 from family NCI-1326. Axial abdominal computed tomography scans from the proband (IV:1, NCI-1326 kindred) following right radical nephrectomy showing multifocal left renal lesions, indicated by arrows in A–D. Subsequently, at the age of 46 years, the individual underwent the first of 3 left partial nephrectomies, for the surgical removal of a 3 cm ccRCC (Fuhrman grade 3), a 1.5 cm ccRCC (Fuhrman grade 3), and a 2 cm atypical cyst with clear cell lining.



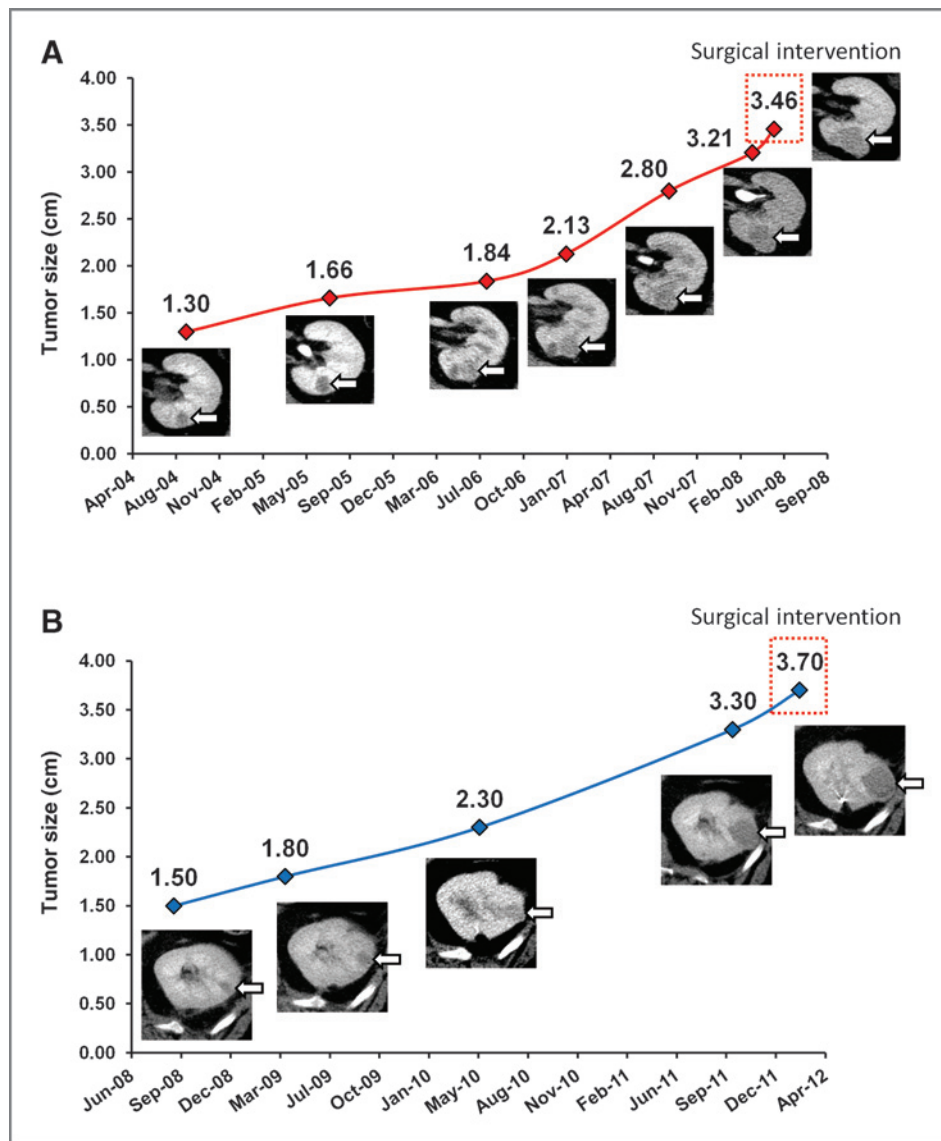


Figure 3. Rapid growth of renal tumors in proband IV:1 from family NCI-1326. Rapid growth rate of proband IV:1 renal tumors before second (A) and third left partial nephrectomies (B).

Given the finding of a *BAP1* missense germline variant (c.41T>A, p.L14H) in individual IV:1, we conducted cosegregation studies. This variant was not found in dbSNP137, Sanger Institute Catalogue of Somatic Mutations in Cancer (COSMIC; ref. 21), or 1000 Genomes Project databases

(13). The same variant was found in germline DNA from affected individual IV:4 (Fig. 5A). In contrast, no germline *BAP1* variant was detected in unaffected individuals IV:3 and IV:5 (Fig. 5A). No DNA could be obtained for individual IV:6 who had died. Thus, the *BAP1* c.41T>A

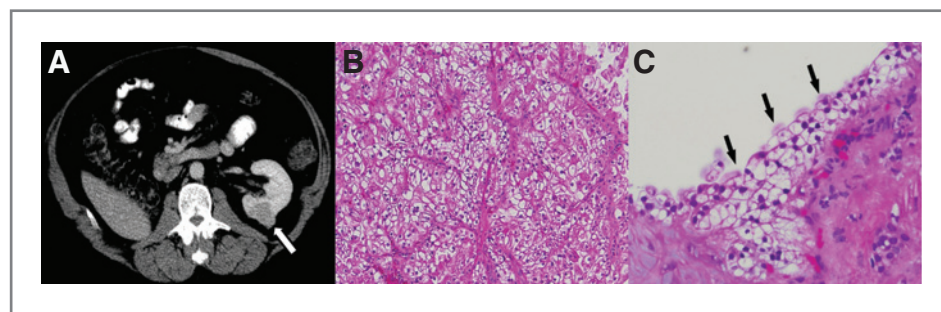
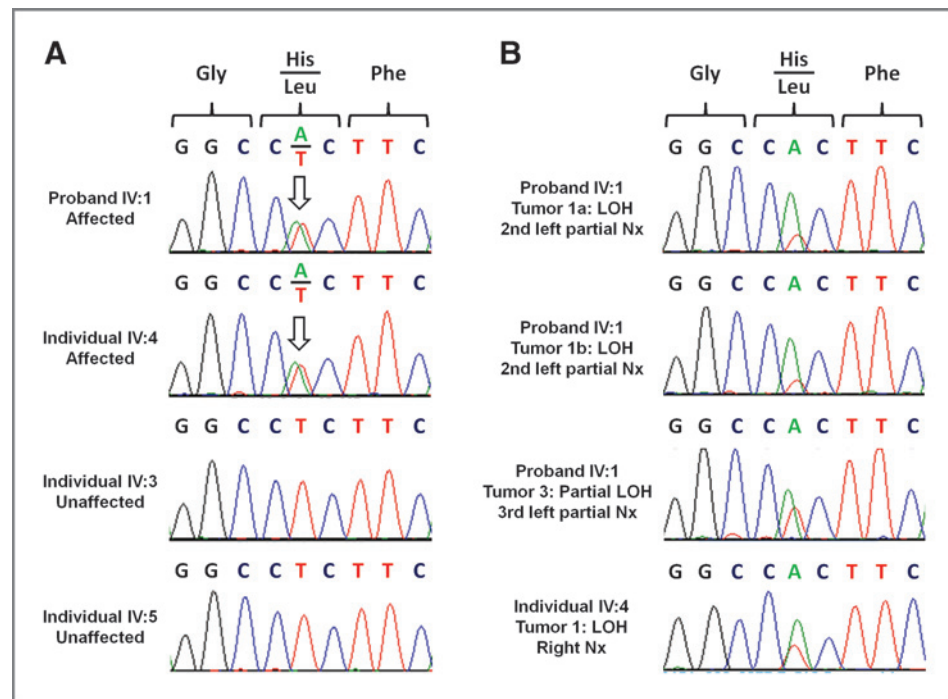


Figure 4. Recurrent multifocal cysts and solid kidney cancer in proband IV:1 from family NCI-1326. A–C, second left partial nephrectomy from proband (IV:1, NCI-1326 kindred). Axial abdominal computed tomography scan (A), and histology slides from removed lesions, a ccRCC (B) and an atypical renal cyst with clear cell lining (arrows; C).

Figure 5. Cosegregation and LOH studies of *BAP1* variant in family NCI-1326. A, sequence chromatogram for proband IV:1 and affected individual IV:4 with the c.41T>A (p.L14H) *BAP1* variant. Unaffected individuals IV:3 and IV:5 were negative for the *BAP1* variant. B, sequence chromatograms of renal tumors from proband IV:1 displaying LOH at the *BAP1* locus for 2 different regions from one tumor (Tumors 1a and 1b) and mutant allele enrichment in another tumor (Tumor 3). Sequence chromatogram of individual IV:4 tumor showing LOH. Nx, nephrectomy.



(p.L14H) variant cosegregated with the RCC predisposition in this family. The odds against random segregation are 5; under a dominant mode of inheritance and assuming full penetrance, the backward odds (22, 23) are 16 and the logarithm of the odds (LOD) score is 1.2.

The *BAP1* variant (p.L14H) maps to the catalytic domain, a domain that is a frequent site of pathogenic missense mutations. Somatic mutations in the ubiquitin C-terminal hydrolase (UCH) domain have been reported in several RCC studies as well as in COSMIC and the Kidney Renal Cell Carcinoma (KIRC) dataset produced by The Cancer Genome Atlas (TCGA) (Fig. 6A; refs. 11, 21, 24). Leucine 14 is highly conserved (Fig. 6B) and along with previously reported RCC mutations in neighboring residues, L14H is predicted to be deleterious by Protein Variation Effect Analyzer (PROVEAN), Sorting Intolerant from Tolerant (SIFT), and PolyPhen-2 prediction tools (Fig. 6C; refs. 19, 25, 26).

We previously constructed a *BAP1* structural model based on the related family members Uch-L3 and Uch37 (11). Leucine 14 maps to the first helix of the UCH domain and is physically adjacent to two previously identified residues subject to pathogenic RCC mutations, p.G13V and p.H144N (Fig. 6D). The leucine 14 side chain in the paralogue UCH-L3 helps organize a crossover loop and other flexible portions of the UCH domain that order upon ubiquitin binding, and forms a portion of the interaction surface for the ULD tail (27). Mutation of this residue to histidine is predicted to increase the effective volume of the side chain, possibly causing steric clashes with surrounding residues, and may prevent productive ubiquitin binding (Fig. 6D).

BAP1 is a two-hit tumor suppressor gene, and we conducted studies for LOH. Three tumors (including 2 samples

from different regions of 1 tumor) were examined from the proband. DNA was extracted from the different tumors and sequenced for the *BAP1* variant (c.41T>A). Two samples from a surgery in 2008 showed clear LOH (Fig. 5B, Tumors 1a and 1b). From a surgery in 2012, 2 tumors were examined. One did not show appreciable LOH, possibly due to contamination by nonmalignant cells or the acquisition of a somatic mutation in the other *BAP1* allele (Tumor 4, data not shown). Enrichment of the mutant allele relative to the wild-type allele was observed in the other tumor from the proband's 2012 surgery (Fig. 5B, Tumor 3). In addition, a tumor was evaluated from individual IV:4. This tumor also showed enrichment of the mutant allele consistent with LOH (Fig. 5B, IV:4 Tumor 1). In addition, *BAP1* protein expression in the tumors was investigated by immunohistochemistry. Immunohistochemical staining was negative for *BAP1* protein in the tumor from individual IV:4 (Fig. 7 and insert A) and Tumors 3 and 4 from the proband (data not shown). For reference, nuclear *BAP1* staining was observed in the normal adjacent epithelium (Fig. 7, asterisk and insert B). All the tumors examined, including Tumor 4 that failed to show LOH at the DNA level, were negative for *BAP1* by immunohistochemistry. Thus, the immunohistochemical data confirm loss of *BAP1* protein and provide further evidence for "two-hit" inactivation of *BAP1* in the tumors from this family. Given that *BAP1* loss by IHC is observed in 15% of sporadic ccRCC (11), the probability that all 3 tumors would be *BAP1* negative by chance alone is 0.0034. These data are most consistent with the notion that (1) p.L14H is a causative mutation, (2) p.L14H abrogates protein expression in tumors, and (3) mutations abolishing expression of the second allele are uniformly present.

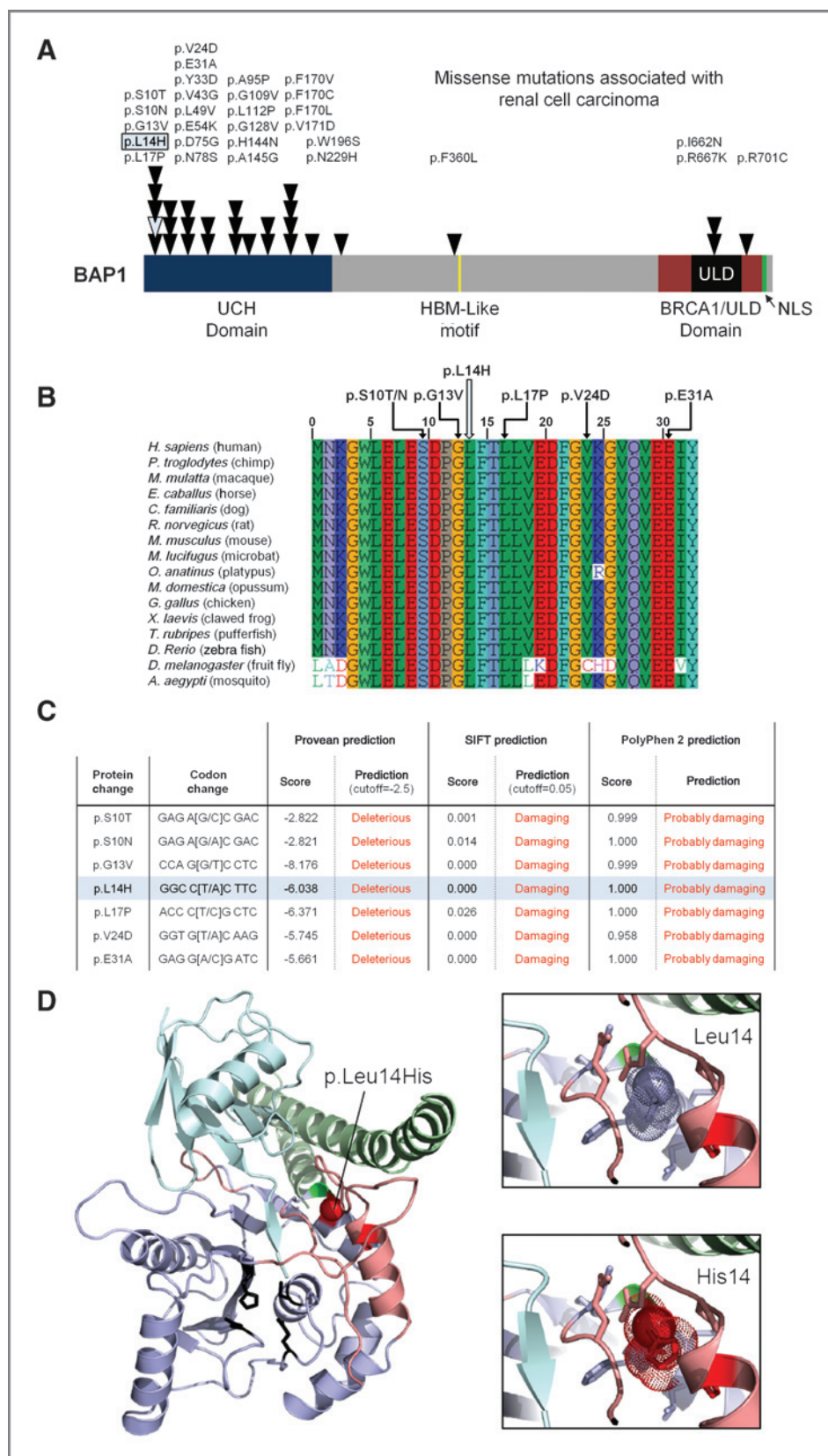


Figure 6. Analysis of the novel p.L14H BAP1 variant. A, schematic of BAP1 protein showing the position of the novel p.L14H missense variant (gray triangle) in comparison with known BAP1 missense mutations associated with sporadic RCC (black triangles). Data compiled from Peña-Llopis and colleagues, Hakimi and colleagues, COSMIC, and KIRC (TCGA; refs. 11, 21, 24). UCH domain (blue); HBM, HCF-1-binding motif (yellow); ULD, Uch37-like domain (black); BRCA1, putative BRCA1-interacting domain (red); NLS, nuclear localization signal (green). B, BAP1 amino acid conservation across species assessed with BioEdit's ClustalW multiple alignment function. Protein sequences are from UniProt (Q92560, H9G0D9, F6TYN2, E2R9Z2, D3ZH56, Q99PU7, G1PS27, F6SMM8, F6RI15, Q5F3N6, Q52L14, H2UEV1, A1L2G3, Q7K5N4, Q17N72) and Ensembl (ENSPTRP00000025898; ref. 33). C, *in silico* predicted effects of the novel p.L14H missense variant and the surrounding sporadic RCC-associated missense mutations assessed with PROVEAN, SIFT, and PolyPhen-2 prediction tools (19, 25, 26). D, BAP1 structure model. Left: cartoon depiction of the BAP1 UCH domain (purple) noting p.Leu14 (red sphere) involved in organizing a flexible crossover loop and other flexible portions of the domain (salmon) that order upon ubiquitin substrate (cyan) binding. Uch37-like domain (ULD) is shown in green. Right top: zoom-in of wild-type BAP1 leucine 14 residue with atom radii depicted in dots interacting with surrounding residues (side chains within 4 Å displayed in stick). Right bottom: zoom-in of BAP1 histidine 14 mutant with atom radii (dots) revealing clashes with surrounding residues.

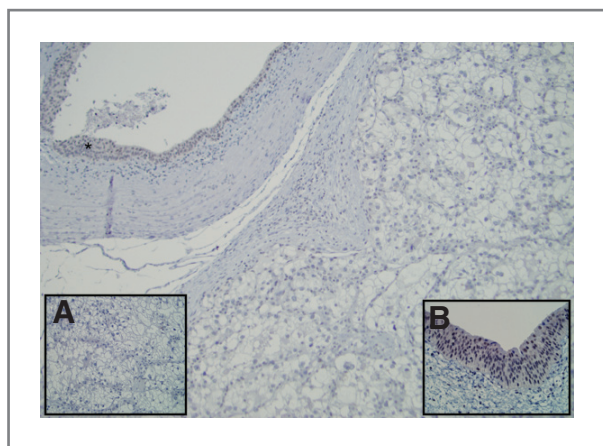


Figure 7. Loss of BAP1 protein in renal tumor from individual IV:4. Low power view of renal tumor from individual IV:4. The tumor involves the medullary area of the kidney and shows negative staining for BAP1. Note the pelvic transitional epithelium that stains positive for BAP1 (*) as positive internal control ($\times 150$). Insert A: high-power image showing the renal tumor with negative BAP1 immunohistochemical staining ($\times 200$). Insert B: high-power image of BAP1 immunohistochemical staining showing pelvic transitional epithelium with positive nuclear staining as a positive internal control ($\times 250$).

Previous *VHL* mutation testing of germline DNA from the proband of family NCI-1326 was negative. However, the *VHL* and *BAP1* genes are both on chromosome 3p so we asked whether somatic mutations in *VHL* could be detected in the tumors. *VHL* mutation analysis (Supplementary Materials and Methods) showed *VHL* mutation in some tumors (IV:1, Tumor 1 and IV:4, Tumor 1), but not in others (IV:1, Tumors 3 and 4; Supplementary Fig. S2 and data not shown). Thus, mutations in *VHL* and *BAP1* may cooperate in the development of at least some tumors.

Together, these data suggest that the novel *BAP1* p.L14H missense variant is the cause of the underlying cancer phenotype in the family described. First, the variant cosegregated with the RCC phenotype. Second, the variant targets the catalytic domain, which is a common site of missense mutations including pathogenic somatically-acquired mutations in neighboring residues p.G13V and p.H144N. Third, L14 is highly conserved across species, and *in silico* analyses suggest that a histidine substitution at this position precludes productive ubiquitin binding. Fourth, consistent with *BAP1* function as a two-hit tumor suppressor gene, the variant was associated with LOH in tumors from the proband and an affected sister by DNA sequence analysis. Finally, albeit indirectly, the absence of BAP1 protein, by immunohistochemistry in all tumors examined, suggests that the *BAP1* p.L14H variant abrogates protein expression. Furthermore, these findings confirm that even in the samples in which LOH was not observed, BAP1 function was lost.

Although it is not possible to generalize from a single kindred, our data suggest that *BAP1* mutations will be found, albeit infrequently, in familial RCC, and thus, it seems fitting to comment on the phenotypic aspects of the family we report. The family in which the novel p.L14H

variant cosegregated with RCC showed a cancer phenotype characterized by an early-onset, aggressive form of ccRCC. The proband is noted to have had bilateral, multifocal disease with multiple solid and cystic lesions with a rapid rate of growth. Individual IV:6 died of early-onset metastatic disease at the age of 36. Two other individuals (II:1 and III:4) died of metastatic RCC at 48 and 58 years of age, respectively. Another family member, who inherited the p.L14H variant, developed early-onset ccRCC at the age of 40 years. Overall, this is consistent with our previous research findings, which have shown an association of *BAP1* loss with high tumor grade and poor survival (11, 12). In addition, other studies have correlated *BAP1* loss with metastases in other *BAP1*-associated cancers, particularly uveal melanoma (9). Taken together, these observations support the idea that germline *BAP1* mutations may be associated with aggressive familial ccRCC.

The NCI-1326 family kidney cancer phenotype is, in some ways, similar to the von Hippel-Lindau (VHL) phenotype, that is, the presence of bilateral, multifocal clear cell tumors and cysts, and tumors within cysts. However, the kidney cancer phenotype in this family seems to differ from the typical VHL phenotype in several ways. The renal tumors in proband IV:1 grew faster than might have normally been expected in a patient with VHL. In the experience at NCI, the average growth rate of VHL-associated RCC is 3 mm per year, which is consistent with the growth rate of sporadic small renal masses (28). In addition, there are a number of high Fuhrman grade ccRCCs in this family, which are uncommonly seen in VHL tumors, particularly those less than 3 cm in size.

There are several clinical implications for the physician when determining a differential diagnosis for germline genetic analysis. Our findings and the fact that somatic *BAP1* mutations are often associated with ccRCC of high grade may encourage clinicians to look for these features when deciding whether to proceed with germline *BAP1* mutation analysis. Identifying cues associated with germline *BAP1* mutation will be important as these mutations are rare. In addition, our family (although not all individuals) displayed a cancer phenotype that was noted to be "VHL-like" with bilateral, multifocal disease and multiple renal cysts. Thus, clinicians may consider *BAP1* analysis for individuals who test negative for germline *VHL* mutations and display a more "aggressive" phenotype that lacks other VHL hallmark findings such as hemangioblastomas, pancreatic cysts, and pheochromocytomas.

Before this report, germline *BAP1* mutations were reported to predispose to several additional cancers including uveal and cutaneous melanoma and mesothelioma (14–17). However, other tumor types have been found in these pedigrees such as lung carcinomas, meningiomas, and cholangiocarcinomas (14, 16–18, 29). We did not observe any of these cancers in our family. The reason for this is unclear. However, these data are in keeping with the previous literature in which, initially, *BAP1* germline mutations were associated with two clinically distinct syndromes of familial melanoma and mesothelioma (17, 18). These separate

cancer phenotypes were later shown to overlap (29, 30). As germline *BAP1* mutation families continue to be described, the phenotype may be clarified. No clear genotype/phenotype correlation has been observed, and familial mutations frequently result in early truncation of the BAP1 protein (14, 15, 17, 18, 29, 31, 32). It seems plausible that germline *BAP1* mutations produce a cancer susceptibility syndrome in which the penetrance of each given feature (RCC, melanoma, or mesothelioma) depends upon additional environmental or genetic factors. Nevertheless, the presence of other BAP1-associated malignancies in RCC families may increase suspicion for a germline *BAP1* mutation.

Although germline *BAP1* mutations may predispose to RCC, the frequency of these mutations is low but in keeping with that of other studies. For comparison, several other studies describing germline *BAP1* mutations in a variety of cohorts describe an overall germline frequency of approximately 3.8% (range of 1.9% in a group of individuals with uveal melanoma to 8.0% in a subset of apparent sporadic mesotheliomas; refs. 14–17, 30). Overall, these data show that germline *BAP1* mutations predispose to several tumor types, and the degree of tumor susceptibility conferred by *BAP1* mutation may vary across tissues.

There are several limitations to this study. First, among the 82 probands successfully evaluated, only one significant *BAP1* variant was found. Second, the functional significance of p. L14H remains to be examined. Third, cosegregation studies could be conducted in just 4 individuals and the LOD score is low. However, given the loss of BAP1 protein by IHC in all tumors examined ($n = 3$) and a probability that this finding would be from chance alone of 0.0034, our results strongly suggest that the variant identified is responsible for the RCC predisposition observed.

In conclusion, we report for the first time a *BAP1* germline missense variant predisposing to familial, early-onset, aggressive ccRCC. Our data suggest that *BAP1* may be the causative gene for renal tumor development in a subset of patients with inherited kidney cancer, although the frequency of *BAP1* gene mutations in RCC families seems to be low.

Disclosure of Potential Conflicts of Interest

No potential conflicts of interest were disclosed.

References

- Pavlovich CP, Schmidt LS. Searching for the hereditary causes of renal-cell carcinoma. *Nat Rev Cancer* 2004;4:381–93.
- Linehan WM. Genetic basis of kidney cancer: role of genomics for the development of disease-based therapeutics. *Genome Res* 2012;22:2089–100.
- Malinoc A, Sullivan M, Wiech T, Kurt Werner S, Jilg C, Straeter J, et al. Biallelic inactivation of the SDHC gene in renal carcinoma associated with paraganglioma syndrome type 3. *Endo Relat Cancer* 2012;19:283–90.
- Ricketts CJ, Shuch B, Vocke CD, Metwalli AR, Bratslavsky G, Middleton L, et al. Succinate dehydrogenase kidney cancer: an aggressive example of the Warburg effect in cancer. *J Urol* 2012;188:2063–71.
- Eletr ZM, Wilkinson KD. An emerging model for BAP1's role in regulating cell cycle progression. *Cell Biochem Biophys* 2011;60:3–11.
- Jensen DE, Proctor M, Marquis ST, Gardner HP, Ha SI, Chodosh LA, et al. BAP1: a novel ubiquitin hydrolase which binds to the BRCA1 RING finger and enhances BRCA1-mediated cell growth suppression. *Oncogene* 1998;16:1097–112.
- Ventii KH, Devi NS, Friedrich KL, Chernova TA, Tighiouart M, Van Meir EG, et al. BRCA1-associated protein-1 is a tumor suppressor that requires deubiquitinating activity and nuclear localization. *Cancer Res* 2008;68:6953–62.
- Bott M, Brevet M, Taylor BS, Shimizu S, Ito T, Wang L, et al. The nuclear deubiquitinase BAP1 is commonly inactivated by somatic mutations and 3p21.1 losses in malignant pleural mesothelioma. *Nat Genet* 2011;43:668–72.
- Harbour JW, Onken MD, Roberson ED, Duan S, Cao L, Worley LA, et al. Frequent mutation of BAP1 in metastasizing uveal melanomas. *Science* 2010;330:1410–3.

Authors' Contributions

Conception and design: M.N. Farley, L.S. Schmidt, W.M. Linehan, J. Brugarolas
Development of methodology: M.N. Farley, L.S. Schmidt, J.L. Mester, S. Peña-Llopis, W.M. Linehan, J. Brugarolas

Acquisition of data (provided animals, acquired and managed patients, provided facilities, etc.): L.S. Schmidt, J.L. Mester, S. Peña-Llopis, A. Pavia-Jiménez, C.D. Vocke, J. Peterson, L. Middleton, A.R. Metwalli, P.L.M. Dahia, C. Eng, W.M. Linehan, J. Brugarolas

Analysis and interpretation of data (e.g., statistical analysis, biostatistics, computational analysis): M.N. Farley, L.S. Schmidt, S. Peña-Llopis, A. Christie, C.D. Vocke, C.J. Ricketts, L. Kinch, N. Grishin, M.J. Merino, C. Xing, X.-J. Xie, P.L.M. Dahia, W.M. Linehan, J. Brugarolas

Writing, review, and/or revision of the manuscript: M.N. Farley, L.S. Schmidt, J.L. Mester, S. Peña-Llopis, A. Pavia-Jiménez, C.D. Vocke, C.J. Ricketts, J. Peterson, A.R. Metwalli, C. Xing, X.-J. Xie, P.L.M. Dahia, C. Eng, W.M. Linehan, J. Brugarolas
Administrative, technical, or material support (i.e., reporting or organizing data, constructing databases): J.L. Mester, A. Pavia-Jiménez, C.J. Ricketts, J. Peterson, C. Eng, W.M. Linehan, J. Brugarolas
Study supervision: M.N. Farley, W.M. Linehan, J. Brugarolas

Acknowledgments

The authors thank the individuals who participated in the study and donated samples, Dr. Payal Kapur for pathologic support and critically reading the manuscript, Dr. Cheryl Lewis for assistance in disseminating phenotypic information from UTSW samples, the staff of the UTSW and Cleveland Clinic Genomic Medicine tissue repositories, Rabindra Gautam for imaging analysis, and Georgia Shaw for assistance with illustrations.

Grant Support

This work was supported by private donations in honor of Mr. Thomas M. Green, Sr. and of a second anonymous patient of Dr. J. Brugarolas as well as grants CPRIT RP101075 and 1P30CA142543. In addition, the work was also supported by grants from the Intramural Research Program of the NIH, NCI, Center for Cancer Research, and was funded, in part, with federal funds from the Frederick National Laboratory for Cancer Research, NIH, under Contract HHSN261200800001E (to L. Schmidt).

The costs of publication of this article were defrayed in part by the payment of page charges. This article must therefore be hereby marked *advertisement* in accordance with 18 U.S.C. Section 1734 solely to indicate this fact.

Appendix

The URLs for data presented herein are as follows:

BioEdit's ClustalW multiple alignment function, <http://www.mbio.ncsu.edu/bioedit/bioedit.html>

Sanger Institute Catalogue of Somatic Mutations in Cancer (COSMIC), <http://www.sanger.ac.uk/genetics/CGP/cosmic>

Ensembl, <http://www.ensembl.org>

PolyPhen-2, <http://genetics.bwh.harvard.edu/pph2>

Protein Variation Effect Analyzer (PROVEAN), <http://provean.jcvi.org/index.php>

Sorting Intolerant from Tolerant (SIFT), <http://sift.jcvi.org>

UniProtKB/Swiss-Prot, <http://www.uniprot.org>

The Cancer Genome Atlas (TCGA), <https://tcga-data.nci.nih.gov/tcga/>

1000 Genomes Project, <http://browser.1000genomes.org/index.html>

Received March 4, 2013; revised April 10, 2013; accepted May 10, 2013; published OnlineFirst May 24, 2013.

10. Guo G, Gui Y, Gao S, Tang A, Hu X, Huang Y, et al. Frequent mutations of genes encoding ubiquitin-mediated proteolysis pathway components in clear cell renal cell carcinoma. *Nat Genet* 2012;44:17–9.
11. Peña-Llopis S, Vega-Rubin-de-Celis S, Liao A, Leng N, Pavia-Jimenez A, Wang S, et al. *BAP1* loss defines a new class of renal cell carcinoma. *Nat Genet* 2012;44:751–9.
12. Kapur P, Peña-Llopis S, Christie A, Zhrebker L, Pavia-Jimenez A, Rathmell WK, et al. Effects on survival of *BAP1* and *PBRM1* mutations in sporadic clear-cell renal-cell carcinoma: a retrospective analysis with independent validation. *Lancet Oncol* 2013;14:159–67.
13. Abecasis GR, Altshuler D, Auton A, Brooks LD, Durbin RM, Gibbs RA, et al. A map of human genome variation from population-scale sequencing. *Nature* 2010;467:1061–73.
14. Abdel-Rahman MH, Pilarski R, Cebulla CM, Massengill JB, Christopher BN, Boru G, et al. Germline *BAP1* mutation predisposes to uveal melanoma, lung adenocarcinoma, meningioma, and other cancers. *J Med Genet* 2011;48:856–9.
15. Aoude LG, Vajdic CM, Krickler A, Armstrong B, Hayward NK. Prevalence of germline *BAP1* mutation in a population-based sample of uveal melanoma cases. *Pigment Cell Melanoma Res* 2012;26:278–9.
16. Njauw CN, Kim I, Piris A, Gabree M, Taylor M, Lane AM, et al. Germline *BAP1* inactivation is preferentially associated with metastatic ocular melanoma and cutaneous-ocular melanoma families. *PLoS ONE* 2012;7:e35295.
17. Testa JR, Cheung M, Pei J, Below JE, Tan Y, Sementino E, et al. Germline *BAP1* mutations predispose to malignant mesothelioma. *Nat Genet* 2011;43:1022–5.
18. Wiesner T, Obenaus AC, Murali R, Fried I, Griewank KG, Ulz P, et al. Germline mutations in *BAP1* predispose to melanocytic tumors. *Nat Genet* 2011;43:1018–21.
19. Adzhubei IA, Schmidt S, Peshkin L, Ramensky VE, Gerasimova A, Bork P, et al. A method and server for predicting damaging missense mutations. *Nat Methods* 2010;7:248–9.
20. Bonne AC, Bodmer D, Schoenmakers EF, van Ravenswaaij CM, Hoogerbrugge N, van Kessel AG. Chromosome 3 translocations and familial renal cell cancer. *Curr Mol Med* 2004;4:849–54.
21. Bamford S, Dawson E, Forbes S, Clements J, Pettett R, Dogan A, et al. The COSMIC (Catalogue of Somatic Mutations in Cancer) database and website. *Br J Cancer* 2004;91:355–8.
22. Barnard GA. Statistical inference. *J Royal Stat Society* 1949;11:115–49.
23. Elston RC. 1996 William Allan Award Address. Algorithms and inferences: the challenge of multifactorial diseases. *Am J Hum Genet* 1997;60:255–62.
24. Hakimi AA, Chen YB, Wren J, Gonen M, Abdel-Wahab O, Heguy A, et al. Clinical and pathologic impact of select chromatin-modulating tumor suppressors in clear cell renal cell carcinoma. *Eur Urol* 2013;63:848–54.
25. Choi Y, Sims GE, Murphy S, Miller JR, Chan AP. Predicting the functional effect of amino acid substitutions and indels. *PLoS ONE* 2012;7:e46688.
26. Ng PC, Henikoff S. SIFT: predicting amino acid changes that affect protein function. *Nucleic Acids Res* 2003;31:3812–4.
27. Misaghi S, Galardy PJ, Meester WJ, Ovaia H, Ploegh HL, Gaudet R. Structure of the ubiquitin hydrolase UCH-L3 complexed with a suicide substrate. *J Biol Chem* 2005;280:1512–20.
28. Chawla SN, Crispen PL, Hanlon AL, Greenberg RE, Chen DY, Uzzo RG. The natural history of observed enhancing renal masses: meta-analysis and review of the world literature. *J Urol* 2006;175:425–31.
29. Wiesner T, Fried I, Ulz P, Stacher E, Popper H, Murali R, et al. Toward an improved definition of the tumor spectrum associated with *BAP1* germline mutations. *J Clin Oncol* 2012;30:e337–40.
30. Carbone M, Yang H, Pass HI, Krausz T, Testa JR, Gaudino G. *BAP1* and cancer. *Nat Rev Cancer* 2013;13:153–9.
31. Hoiom V, Edsgard D, Helgadottir H, Eriksson H, All-Ericsson C, Tuominen R, et al. Hereditary uveal melanoma: a report of a germline mutation in *BAP1*. *Genes Chromosomes Cancer* 2013;52:378–84.
32. Wadt K, Choi J, Chung JY, Kiilgaard J, Heegaard S, Drzewiecki KT, et al. A cryptic *BAP1* splice mutation in a family with uveal and cutaneous melanoma, and paraganglioma. *Pigment Cell Melanoma Res* 2012;25:815–8.
33. Flicek P, Amode MR, Barrell D, Beal K, Brent S, Carvalho-Silva D, et al. Ensembl 2012. *Nucleic Acids Res* 2012;40:D84–90.